ELSEVIER

Journal of Molecular Catalysis A: Chemical 188 (2002) 233–243

JOURNAL OF MOLECULAR CATALYSIS A: CHEMICAL

www.elsevier.com/locate/molcata

Kinetic study of *n*-heptane conversion on sulfated zirconia-supported platinum catalyst: the metal–proton adduct is the active site

Ümit Bilge Demirci, François Garin*

Laboratoire des Matériaux, Surfaces, et Procédés pour la Catalyse (LMSPC), UMR 7515-CNRS, ECPM, Université Louis Pasteur, 25 rue Becquerel, 67087 Strasbourg Cedex 2, France

Received 3 April 2002; accepted 3 June 2002

Abstract

Isomerization and cracking reactions of *n*-heptane on 0.2 wt.% platinum supported on sulfated zirconia (Pt/SZ) are investigated in such a way to get maximum kinetic data. The experimental conditions were varied as follows: (i) two ranges of hydrogen pressure, low pressure (LP) 190–760 Torr and high pressure (HP) 900–3000 Torr were studied; (ii) reaction temperatures of 150, 200 and 250 °C were investigated; and (iii) hydrocarbon partial pressures from 5 to 40 Torr were analyzed. Reaction orders versus hydrogen pressure and hydrocarbon pressure, and apparent activation energy values have been determined. The Pt/SZ catalyst displays an original catalytic behavior: (i) at LP, the hydrogen reaction order is negative, while it is positive at HP, and in both cases, these orders tend towards zero when the reaction temperature increases; (ii) the apparent activation energy values are lower at HP than at LP; and (iii) the reaction orders versus hydrocarbon are equal to 1 whatever the experimental conditions are. The changes in the experimental conditions involve modifications of the kinetic parameters. Such results are explained by the fact that the relative proportions of metallic sites or acid sites are influenced by the experimental conditions. The metal–proton adduct site $[H–(M_m)(H^+)_x]^{x+}$ explains these experimental results. We interpret that at hydrogen pressures higher than 760 Torr, the excess of hydrogen provokes a shift in the reactivity from the metallic part of the adduct to the acid one. In fact, at HP and at high reaction temperature, the reactivity is controlled by the acid sites, while at LP and low temperature, it is managed by the metallic and the acid sites.

Keywords: Sulfated zirconia-supported platinum; Metal–proton adduct; Bifunctional mechanism; Kinetic data; Hydrogen effect

1. Introduction

Sulfated zirconia (SZ) is a solid acid catalyst, which is able to catalyze isomerization reaction of alkanes, and particularly, *n*-butane isomerization into *iso*-butane at low temperatures [1]. Despite its high acidity or superacidity, as it is sometimes called [1,2], this catalyst deactivates rapidly [3]. The addition of a metal, like platinum [4–6], increases its stability. Furthermore, the simultaneous presence of hydrogen and platinum is essential to have a stable active catalyst [6–8], even if Garin et al. [4] showed that Pt addition to SZ has no influence on the catalyst stability and activity in presence of sufficiently high hydrogen pressure.

Platinum supported sulfated zirconia (Pt/SZ) is a bifunctional catalyst, with a metallic function, Pt, and

* Corresponding author. Tel.: +33-3902-42737; fax: +33-3902-42761.
E-mail address: garin@chimie.u-strasbg.fr (F. Garin).

1381-1169/02/$ – see front matter © 2002 Elsevier Science B.V. All rights reserved.
PII: S1381-1169(02)00337-0

an acidic function, SZ. Generally, on a bifunctional catalyst, the isomerization reaction is believed to proceed, following the "traditional" bifunctional mechanism, proposed by Mills et al. [9], which comprises the dehydrogenation of alkanes on the metal surfaces, the isomerization of the protonated alkenes on the acid sites, and the hydrogenation of the isomerized alkenes on the metal surfaces.

However, recent investigations have introduced some modifications to this mechanism. In our previous paper [10], we suggested the presence of a metal–proton adduct $[H–(M_m)(H^+)_x]^{x+}$, to explain our results concerning the conversion of nC$_7$, nC$_8$ and nC$_9$ on Pt, Ir, or Pd supported on SZ. This adduct site combines metallic and acidic sites, and consequently, the migration step between these two sites is suppressed. This concept is in agreement with the $[Pd_nH]^+$ and $[Pt_nH]^+$ adducts, which act as "collapsed bifunctional sites", as proposed by Sachtler and coworkers [11–14], and also, with the "compressed bifunctional sites" suggested by Paál and coworkers [15,16] paraphrasing the preceding authors.

Many investigations, concerning the properties and characteristics of SZ and Pt/SZ, have been published. But the results are much debated. Particularly, the reaction mechanisms and the role of hydrogen are controversial. Iglesia et al. [17] supposed that Pt catalyzes the molecular hydrogen dissociation as hydride and proton. The proton acts then as a Brønsted acid site, while the hydride reacts with the isomerized carbenium ion to form the product, decreasing the surface lifetime of this ion. Hattori and coworkers [5,18–20] and Tomishige et al. [7] suggested an other interpretation. They think that H_2, adsorbed on Pt, is dissociated in atomic hydrogens, which undergo by spillover onto the SZ and convert to a proton and a hydride, the former one acting as an active site. Concerning the nC$_4$ isomerization reaction, Garin et al. [21] suggested that the isomerization follows a monomolecular mechanism, while Sachtler and coworkers [13,22–24] proposed that the predominant mechanism is the intermolecular one, supposing the formation of a C_8^+ as reaction intermediate. However, according to Tran et al. [25], this difference in butane isomerization mechanism is mainly due to the nature of the gas used in the experiments, N_2 or H_2. Tran et al. [25] showed that the isomerization follows a bimolecular process under nitrogen, and that hydrogen has an inhibition effect on this mechanism and favors monomolecular processes. This observation reinforces the explanations of our results [21].

Kinetic studies can provide informations concerning the H_2 role and the catalyst's behavior. In general, a conventional bifunctional metal-acid catalyst exhibits specific kinetic data: (i) hydrogen reaction orders between −1 and 0; (ii) hydrocarbon reaction orders close to 1; and (iii) apparent activation energy values between 20 and 30 kcal/mol [26–29]. But, concerning the Pt/SZ catalyst, the hydrogen reaction orders differ from one paper to the other. In some studies, negative values are found [7,23,30], while in others, the orders are positive [17,31–33]. In both cases, the reactions are performed at temperatures higher than 150–200 °C and at hydrogen pressure superior to atmospheric pressure. However, in a general manner, a hydrogen–inert gas mixture is used in the former case, while pure hydrogen is the gas vector in the latter situation. Different interpretations are then provided to explain these orders, besides the fact that the reactions were realized under different conditions.

This paper reports a kinetic study, of *n*-heptane conversion on 0.2 wt.% Pt-supported sulfated zirconia, under low (190–760 Torr) and high (900–3000 Torr) hydrogen pressures. This study gives information about the catalyst behavior in relation to hydrogen concentration.

2. Experimental

2.1. Catalyst preparation

A one step sol–gel synthesis of sulfated zirconia was used [34,35]. It consisted in addition of water to alcohol solution (*n*-propyl alcohol) of zirconium alkoxide (zirconium *n*-propoxide), the sulfuric acid being introduced through the hydrolysis water. The solid was dried at 80 °C for 18 h and calcined at 625 °C for 4 h. Then 0.2 wt.% of platinum was added from $Pt(NH_3)_4(NO_3)_2$. The mixture was stirred for 2 h and then was dried in an oven for 12 h. The hydrogen reduction was performed at 350 °C for 2 h.

The sulfur content of the support was equal to 1.14 wt.%. The BET of the support was equal to 81 m^2/g. After calcination at 625 °C, amorphous-sulfated zirconia crystallized in the tetragonal phase.

2.2. Apparatus, procedure and calculation

The catalytic reactions at low and atmospheric pressures were carried out in a pulse flow system with a glass-fixed bed reactor working at atmospheric total pressure. In each run 5 μl of *n*-heptane (Fluka, puriss. standard for GC) were introduced into the gas flow of hydrogen–helium mixture (Air liquide, purity 4N) at constant hydrocarbon partial pressure (around 5 Torr) thanks to a cooled trap kept at a constant temperature. The hydrogen partial pressure was varied from 190 to 760 Torr.

For the experiments at high pressures, the catalytic reactions were also carried out in a pulse flow system with a fixed bed reactor, but this device is different of the precedent. It is made in stainless steel, but the reactor consists of a glass tube inserted in the stainless steel reactor tube. The hydrogen pressure was varied from 900 to 3000 Torr. In each run, 5 μl of *n*-heptane were introduced into the gas flow of hydrogen at constant hydrocarbon partial pressure (around 5 Torr) thanks to a cooled trap kept at a constant temperature. We have to notice here that the use of a stainless steel reactor tube without an inner glass tube leads to the deactivation of the catalyst. The reaction rate is divided by about a factor of 100 in comparison to the rates obtained in presence of the glass reactor. It seems that the sulfates of the Pt/SZ catalyst are decomposed and attack the inner side of the stainless steel tube during the catalyst activation process.

In both cases, the products were analyzed by gas chromatographs (Varian 3300) equipped with a flame ionization detector and a capillary column (CP Sil 5CB, length 50 m, diameter 0.53 mm). The GCs were always coupled to the outlet of the catalytic reactors, and we have defined:

- the total conversion α_T in percent as:

$$\alpha_T\,(\%) = 100 - \text{amount of unreacted reactant}$$

- the isomerization selectivity, S_{isom} (%) as:

$$S_{isom}\,(\%) = \frac{100 \times \sum \text{isomer formed}}{\sum \text{isomer formed} + \sum \text{cracked products}} \quad (1)$$

The denominator of Eq. (1) is equal to α_T (%); and all the calculations are in moles.

2.3. Kinetic study

In such a way to get a maximum of information, the experiments were performed as follows. For hydrogen order determinations, the pressure of hydrogen varied when reaction temperature and hydrocarbon pressure (around 5 Torr) were kept constant. Two domains of hydrogen pressures were investigated: one between 190 and 760 Torr and the other one between 900 and 3000 Torr. The hydrogen orders were determined, in these two domains of pressure, at three different temperatures: 150, 200 and 250 °C. The hydrogen flow was of 30 and 100 ml/min, for the experiments led at 150 and 200–250 °C, respectively. For the hydrocarbon order measurements, hydrogen pressure and reaction temperature were kept constant, the hydrocarbon pressures varied between 5 and 40 Torr. These experiments were performed at three different temperatures 170, 180, and 240 °C and at three different hydrogen pressures 760, 1500, and 2250 Torr. The hydrogen flow was of 30 and 100 ml/min, for the experiments led at 170–180 and 240 °C, respectively. Finally, the apparent activation energy values were determined between 150 and 250 °C at $P(H_2) = 760$, 1500 and 2250 Torr with $P(nC_7) = 5$ Torr. The hydrogen flow was settled to 100 ml/min.

The reaction rates r (nmol/(g s)) were determined by the following equation:

$$r = \frac{Vd}{M\omega t} \ln\left(\frac{1}{1-\alpha_T}\right)$$

where V is the hydrocarbon volume injected (l), d the hydrocarbon density (g/l), M the hydrocarbon molar weight (g/mol), ω the weight of catalyst (g), and t the time for the hydrocarbon to pass throughout the catalyst (s). The isomerization rate, r_{isom}, and the cracking rate, r_{crack}, are determined according to this equation, but in replacing, respectively, α_T by $\alpha_{isom} = \alpha_T S_{isom}$ and by $\alpha_{crack} = \alpha_T S_{crack}$, with α_{isom} the conversion in isomer products, S_{isom} the fraction of isomers formed among the reaction products, α_{crack} the conversion in cracked products, and S_{crack} the fraction of cracked products formed among the reaction products. In all the experiments, for the determination of the kinetic data, the total conversion α_T was <25%. This was performed by adjusting the gas flow, as mentioned.

Table 1
Reaction orders vs. hydrogen pressure ($P(nC_7) = 5$ Torr)

T (°C)	Low P (H_2) (190–760 Torr)	High P (H_2) (900–3000 Torr)	Δn (H_2)[a]
150	−0.50	0.80	1.30
200	−0.35	0.20	0.55
250	−0.15	0.00	0.15

[a] Gaps between the orders at low pressures and the orders at high pressures.

Table 2
Reaction orders vs. nC_7 partial pressure

T (°C)	P (H_2) (Torr)	P (nC_7) (Torr)	Reaction order in nC_7
170	760	5–45	1.00
180	760	5–29	0.95
240	760	5–40	1.00
240	1500	5–40	1.00
240	2250	5–40	1.00

3. Results

The reaction rate r, in general, can be written following a power law $r = kP(H_2)^n P(nC_7)^m f$ (state of the catalyst), where $k = Ae^{-E_A/RT}$, and we determined n, m and E_A.

3.1. Hydrogen reaction orders

Table 1 shows the different reaction orders versus hydrogen pressure, obtained at 150, 200 and 250 °C, and, for each case, at two different ranges of hydrogen pressures: (i) low pressures (LP), 190–760 Torr; and (ii) high pressures (HP), 900–3000 Torr. From Table 1, we can remark different points:

(i) at a given temperature, the orders at LP and HP are negative and positive, respectively, but at 250 °C and at HP, the order is zero,
(ii) increasing the reaction temperature, the orders at LP and HP increase and decrease, respectively towards zero value,
(iii) the gaps between the orders at LP and HP diminish with the increase of the temperature: 1.30 at 150 °C, 0.55 at 200 °C, and 0.15 at 250 °C,
(iv) at 150 °C, the influence of hydrogen is the most important. At 250 °C, the hydrogen pressure has a small effect on the reaction rate at LP, and no influence at HP. The orders obtained at 200 °C correspond to intermediate values.

3.2. Reaction orders versus n-heptane partial pressure

The reaction orders versus nC_7 partial pressures have been settled, firstly at atmospheric pressure of hydrogen and at three different temperatures, 170, 180, and 240 °C, and, secondly at 240 °C for three different hydrogen pressures 760, 1500, and 2250 Torr (Table 2). In each case, the order values are very close to 1. The reaction rate is then proportional to the nC_7 partial pressure, independently of the reaction temperature and of the total pressure.

3.3. Apparent activation energy data

The global apparent activation energy (E_A) and the apparent activation energy values for isomerization and cracking reactions (E_A^{isom} and E_A^{crack}, respectively) have been determined graphically in a range of temperatures from 150 to 250 °C, and at three different hydrogen pressures, 760, 1500, and 2250 Torr (Table 3). For these three experiments, the E_A^{crack} are greater than the E_A^{isom}. At 1500 and 2250 Torr, E_A^{crack} has the same value, approximately 32.5 kcal/mol, while E_A^{isom} is slightly different and close to 12 kcal/mol. At

Table 3
Apparent activation energy values ($P(nC_7) = 5$ Torr)

Experimental conditions		Global E_A (kcal/mol)	Isomerization E_A^{isom} (kcal/mol)	Cracking E_A^{crack} (kcal/mol)
T (°C)	P (H_2) (Torr)			
150–250	760	31.0 ± 0.5	28.0 ± 1.5	38.0 ± 0.5
150–250	1500	19.0	12.5	32.5
150–250	2250	18.5	11.5	32.5

atmospheric pressure, the apparent activation energy values are similar to those corresponding to a reaction performed on a bifunctional catalyst. However, at higher hydrogen pressures, they are lowered. On one hand, E_A^{isom} has values almost divided by two from the one obtained at atmospheric pressure. On the other hand, E_A^{crack} is decreased by few units (32.5 kcal/mol versus 38.0 kcal/mol at atmospheric pressure). Moreover, the global apparent activation energy values show the same evolutions.

4. Discussion

Contrary to homogeneous gas-phase reactions, reactions between gases catalyzed by metals often exhibit a negative pressure dependency on the partial pressure of one of the reactants, even under initial conditions. This is frequently the case for hydrogen in catalytic reactions involving hydrocarbons such as in hydrogenolysis and isomerization reactions.

In most of the interpretations of the negative order relative to H_2 pressure, in reactions of alkanes, it is striking that the inhibiting effect in H_2 pressure is related to the degree of dehydrogenation of the most abundant surface intermediate. When analyzing the experimental data concerning catalytic reactions of alkanes on metals, it appears that the value of the inhibiting effect in hydrogen pressure is not independent of the experimental conditions [36]: it varies continuously with both temperature and pressure ranges. In fact, on pure metals, that inhibiting effect is increasing both when the H_2 pressure increases and when the temperature is lowered. This, of course, leads to the difficulty that the degree of dehydrogenation should increase when the H_2 pressure is increased or when the temperature is lowered [37]. Moreover, our results do not follow exactly those obtained on pure metals. At low hydrogen pressure, when decreasing the reaction temperature, the inhibiting effect is increasing as already noticed but at high hydrogen pressure, it is no longer the case, a promoting effect takes place, which is more important at low temperature than at high temperature.

Generally, for conventional bifunctional metal-acid catalysts as, Pt/MOR [26], Pt/SiO_2–Al_2O_3 [27], Pt/$AlCl_3$–Al_2O_3 [28] and Pt/HMOR [29], in all the pressure range studied, between 200 and 3000 Torr, the order versus hydrogen is always negative. Then it shows that Pt/SZ has a particular behavior:

(i) At low hydrogen pressure, H_2 has an inhibiting effect (Table 1).
(ii) At high hydrogen pressure, H_2 has a promoting effect (Table 1).
(iii) The hydrogen reaction orders are dependent on the reaction temperature: at low and high pressures, they respectively increase and decrease towards zero value when the temperature is enhanced (Table 1).
(iv) As reported in our previous paper [10], at atmospheric pressure, the isomerization selectivity increases, at isoconversion, with reaction temperature (from 200 to 250 °C). This particular evolution was attributed to the participation of a metal–proton adduct site in the isomerization reaction. However, at high hydrogen pressure, the isomerization selectivity drops, at a given total conversion, with increasing reaction temperature (Fig. 1): at $\alpha_T \sim 20\%$, $S_{isom} \sim 70\%$ at 150 °C, while $S_{isom} \sim 50\%$ at 200 °C; and, at $\alpha_T \sim 60\%$, $S_{isom} > 40\%$ at 200 °C, while $S_{isom} < 30\%$ at 250 °C. This behavior is characteristic of an acid catalyzed reaction. On metallic catalysts, when

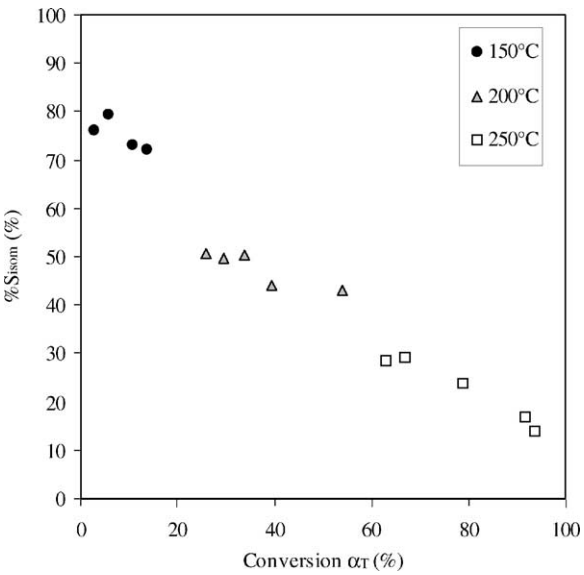

Fig. 1. Reactivity of *n*-heptane on Pt/SZ at a hydrogen pressure of 1500 Torr. Evolution of the isomerization selectivity S_{isom} (%) as a function of the total conversion α_T, at three different temperatures.

the reaction temperature is increased, the relative contribution of the isomers is increased. This is due to the fact that $E_A^{isom} > E_A^{crack}$. These results were obtained on 10 and 0.2 wt.% Pt on γ-Al_2O_3 catalysts [38–40]. Furthermore, the transition from low pressure to high pressure is characterized by a small decrease in the reaction rate (Fig. 2). At 150 °C, the reaction rates are 3.43×10^{-11} and 1.79×10^{-11} nmol/(g s), respectively, at 760 and 900 Torr. The rate is divided by a factor 2. This loss of activity is slightly more important at 150 °C than at 250 °C. It can be explained by poisoning of the metallic part of the metal–proton adduct.

In summary, hydrogen reaction orders vary, on one hand, with the hydrogen pressures, and on the other hand, with the reaction temperatures. Moreover, it seems that there is a transition from a metal-acid bifunctional catalysis to an acid catalysis with the increase of either hydrogen pressure or reaction temperature.

Following the Frennet's concept [37,41,42] concerning the fact that the active sites for adsorption, the landing site, and for the reaction involve an ensemble of $Z_{surf.\,at.}$ surface atoms, the rate equation of that adsorption step r_{ads} can be written as follows:

$$C_nH_{2n+2} + H_{ads} + Z_{surf.\,at.}S \rightarrow$$

$$r_{ads} = k_{ads} P_{HC} \theta_H \theta_S{}^Z \qquad \text{where} \quad \theta_H + \theta_S + \theta_C = 1$$

with k_{ads} the rate constant of the adsorption step, P_{HC} the hydrocarbon partial pressure, θ_H the fraction of adsorbed hydrogen atoms, θ_S the fraction of free surface sites S, and θ_C the fraction of adsorbed hydrocarbon molecules. H_{ads} is a chemisorbed hydrogen atom in adsorption–desorption equilibrium with the gaseous hydrogen. This associative adsorption process can explain very high hydrogen inhibiting values without deeply dehydrogenate the most abundant surface intermediate [43]. In fact, the hydrogen order value is a function of the ensemble Z of surface atoms, and the

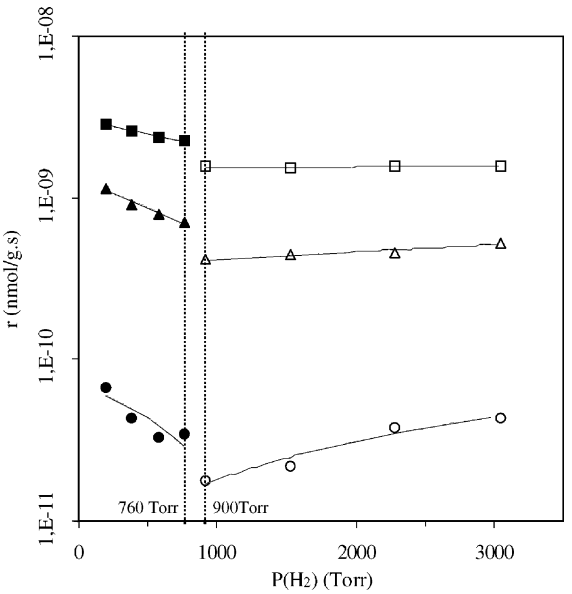

Fig. 2. *n*-Heptane reactivity on Pt/SZ. Evolution of the reaction rates as a function of the hydrogen pressure (the hydrocarbon pressure is kept constant at 5 Torr), at three different temperatures: 150 °C (circle); 200 °C (triangle); 250 °C (square) (in white, low pressures; in black, high pressures).

active site is composed of adsorbed hydrogen and of Z free surface atoms. This concept is very close to our proposal concerning the active sites in bifunctional catalysis where is involved a metal–proton adduct $[(Pt_m)(H^+)_x]^{x+}$ as active site, as reported in our previous paper [10]. This site groups together the acidic and the metallic functions. Then the alkane isomerization is visualized taking place on such sites without the need for the intermediates to shuttle between metal and acid sites. All the reaction steps can be achieved during a single residence of the molecule. The adsorption step is associative, and as the experiments are performed under an excess of hydrogen, some hydrogen atoms are adsorbed on the metallic sites. The reactive site is then $[H–(Pt_m)(H^+)_x]^{x+}$. The following general reactions were suggested [10]:

$$\begin{aligned}
&C_nH_{2n+2} + [(H–Pt_m)(H^+)x]^{x+} \leftrightarrow [C_nH_{2n+3}]_{\text{Pt participation}\,\text{agostic species (A)}}\\
&[C_nH_{2n+3}]_{\text{Pt participation}\,\text{agostic species (A)}} \leftrightarrow [C_nH_{2n+3}]^+_{\text{acid participation}\,\text{carbonium ion(B)}}\\
&[C_nH_{2n+3}]^+_{\text{acid participation}\,\text{carbonium ion(B)}} \leftrightarrow [C_nH_{2n+1}]^+_{\text{(Pt+acid) participations}} + H_2{}_{\text{carbenium ion (C)}}\\
&[C_nH_{2n+1}]^+_{\text{(Pt+acid) participations}\,\text{carbenium ion (C)}} \rightarrow \text{isomers or cracked products}
\end{aligned} \qquad \text{(I)}$$

Table 4
Cracking product distributions from nC_7 on 0.2 wt.% Pt/SZ, obtained at reaction temperatures of 150, 200 and 250 °C, and at hydrogen pressures of 760 Torr [10] and 2250 Torr

P (H_2) (Torr)	T (°C)	α_T (%)	S_{isom} (%)	Cracking products selectivity (%)		
				C_3	iC_4	nC_4
760	150	19.6	64.9	18.1	17.0	0.0
760	200	23.8	15.5	43.8	40.3	0.4
760	250	19.3	70.5	15.1	14.0	0.4
2250	150	13.7	72.1	14.4	13.5	0.0
2250	200	19.7	50.7	25.8	23.5	0.0
2250	250	15.6	32.8	34.1	33.1	0.0

The Eq. (I) follows the Eley–Rideal kinetic model. The reactant adsorbs on the metallic part of the adduct site and an agostic species (A) is formed. An equilibrium occurs between (A) and a carbonium ion (B) formed with the proton of the acidic part of the adduct site. Finally, a carbenium ion (C) is formed giving isomers and/or cracked products. At that point, we have to point out that the cracking pattern is very simple. The amount of C_3 equals to the iC_4 formed (Table 4). Methane, ethane, pentanes and hexanes are not produced. Moreover, at low conversions ($\alpha_T < 25\%$), the isomerization selectivity is independent of the total conversions and remains almost constant [10], around 75% at 150 °C and around 45% at 200 °C (Fig. 1). The formation of cracked products is then a parallel reaction with respect to isomerization. However, at higher conversions ($\alpha_T > 25\%$), the isomerization selectivity decreases with increasing conversion, as observed on Fig. 1 and at 250 °C [10]. Hence, cracked products are also formed by a consecutive reaction which is added to the simultaneous reactions [10].

4.1. Inhibiting effect of hydrogen at low pressures

At 150 °C, the hydrogen pressure has a negative effect on the catalyst activity and at such temperature the metal is only reactive for carbon–hydrogen bond breaking. In agreement with our bifunctional mechanism, the rate determining step is then the reaction occuring on the acid site of the adduct. The reaction sequences, as given, can be written as follows:

$$C_nH_{2n+2} + (H_{ads} + Z_{surf.\,at.}S) \leftrightarrow [C_nH_{2n+3}]_{Pt} \quad (K_1)$$

$$[C_nH_{2n+3}]_{Pt} \leftrightarrow [C_nH_{2n+3}]^+_{acid} \quad (K_2)$$

$$[C_nH_{2n+3}]^+_{acid} \leftrightarrow [C_nH_{2n+1}]^+_{(Pt+acid)} + H_2 \quad (K_3)$$

$$[C_nH_{2n+1}]^+_{(Pt+acid)} \rightarrow \text{isomers or cracked products} \quad (k)$$

where K_1 is the adsorption equilibrium constant on the metal, K_2 the carbonium formation equilibrium constant, K_3 the carbonium dehydrogenation equilibrium constant, and k the rate constant on the acid function. According to the Frennet's concept [37,41,42], the adsorbed hydrogen on an ensemble of $Z_{surf.\,at.}$ surface atoms ($H_{ads} + Z_{surf.\,at.}$ S) can be seen as the "hydrogen–platinum–proton" adduct $[H–(Pt_m)(H^+)_x]^{x+}$ where m is the size of the metallic aggregate.

The rate equation r is:

$$r = k[C_nH_{2n+1}]^+_{(Pt+acid)}$$

$$K_1 = \frac{[C_nH_{2n+3}]_{Pt}}{P_{HC}\theta_H(\theta_S)^Z} \qquad K_2 = \frac{[C_nH_{2n+3}]^+_{acid}}{[C_nH_{2n+3}]_{Pt}}$$

$$K_3 = \frac{[C_nH_{2n+1}]^+_{(Pt+acid)}P_{H_2}}{[C_nH_{2n+3}]^+_{acid}}$$

with $\theta_S+\theta_C+\theta_H = 1$, $\theta_H = \theta^0_H(1-\theta_C)$, and $\theta_S = (1-\theta^0_H)(1-\theta_C)$ where θ^0_H characterizes the H_2 coverage in the absence of chemisorbed hydrocarbon radicals [37,41]. Therefore, the global rate expression can be written as:

$$r = kK_1K_2K_3P_{HC}\theta^0_H(1-\theta_C)^{Z+1}(1-\theta^0_H)^Z(P_{H_2})^{-1} \quad (2)$$

The hydrocarbon reaction order is equal to 1, whatever the hydrogen pressure and the reaction temperature are (Table 2). At low hydrogen pressure the metallic behavior predominates, at least for the adsorption step, hence the fraction of adsorbed hydrocarbon can be neglected, $\theta_C \approx 0$. Furthermore, the fraction of adsorbed hydrogen can be assumed to be low $(1-\theta^0_H) \approx 1$ and then $\theta^0_H \approx (K_HP_{H_2})^{1/2}$, K_H being the equilibrium constant of molecular hydrogen dissociation [41]. Thus, at low hydrogen pressure the rate equation can be written as:

$$r = kK_1K_2K_3K_H^{1/2}P_{HC}(P_{H_2})^{-1/2} \quad (3)$$

This equation gives a hydrogen reaction order of −0.5, which is similar to our experimental value obtained at 150 °C (Table 1).

As observed, the hydrogen reaction order depends of the reaction temperature: it increases from −0.50 to −0.15 when the temperature is raised from 150 to 250 °C (Table 1). These results point out that the participation of the acidic function is more and more pronounced as the temperature is increased.

Negative orders versus hydrogen were already observed by Sachtler and coworkers [23], where $n(H_2) = -1.1$ to -1.3 for nC_4 isomerization on Pt/SZ. For nC_5, the order was −0.15 [24]. Otherwise, Sayari et al. [30] observed a negative order in hydrogen of −1.2 for butane conversion on SZ at 180 °C. Tomishige et al. [7] investigated the nC_4 isomerization at high temperatures 220–400 °C and in a large range of hydrogen pressures 1–50 bar. In all cases, the reaction order was negative.

4.2. Promoting effect of hydrogen at high pressures

At hydrogen pressures higher than atmospheric pressure, the hydrogen reaction order shows positive values (Table 1). Hydrogen pressure has a positive effect on the reaction rate. In this range of pressure, it has been noticed, that the reaction seems to be more driven by the acid sites. Following our bifunctional mechanism, the active sites are metal–proton adducts, where are distinguished metallic and acidic functions. We suggest a competition between these two functions. In this situation, contrary to the low pressure's case, the fraction of adsorbed hydrocarbon θ_C is no longer negligible as the reaction is performed via acid sites, for which the adsorption is stronger than on metals. Moreover, we observed that the reaction rate is decreased under such experimental conditions (Fig. 2). The hydrocarbon adsorption can be defined as:

$$C_nH_{2n+2} + H_{ads} \overset{k_1}{\underset{k_2}{\leftrightarrow}} (C_nH_{2n+3-2\delta})_{ads} + \delta H_2$$

At equilibrium, $k_1 P_{HC}\theta_H = k_2 (P_{H_2})^{\delta}\theta_C$, and $\theta_C = K_C P_{HC}(P_{H_2})^{-\delta}/1 + K_C P_{HC}(P_{H_2})^{-\delta}$, where $K_C = k_1/k_2\,\theta_H^0$. Then, we can approximate $(1-\theta_C)$ as $(1-\theta_C) \approx \frac{(P_{H_2})^{\delta}}{K_C P_{HC}} \approx K'_C (P_{H_2})^{\delta}(P_{HC})^{-\beta}$ [41,44,45], where β is defined in a way to moderate the inhibiting hydrocarbon effect, and δ is related to the degree of dehydrogenation of the hydrocarbon residues [37,44,45]. Moreover, at high hydrogen pressure, $\theta_H^0 \approx 1$, and $(1-\theta_H^0) \approx (K_H P_{H_2})^{-1/2}$ [41]. Therefore, the Eq. (2) becomes:

$$r = kK_1K_2K_3K_H^{-Z/2}K'^{(Z+1)}_C (P_{HC})^{1-\beta(Z+1)} \times (P_{H_2})^{\delta Z - Z/2 + \delta - 1} \quad (4)$$

The hydrogen reaction order is equal to $Z/2$, with $\delta = 1$. At high hydrogen pressure and at 150 °C, we have a hydrogen reaction order of +0.80 (Table 1). From this result, we can deduce a value for Z approximately equal to 2. This value is in agreement with our reaction scheme, which needs two free sites: one located on the metal (hydrocarbon adsorption), and the other on the acid site (hydrocarbon activation by a proton).

Furthermore, if the inhibiting hydrocarbon effect is low, i.e. $\beta \sim 0$, then the order versus the hydrocarbon is almost equal to 1 as observed experimentally.

The temperature increase involves a decrease in hydrogen reaction order toward zero (Table 1), which can be explained by the presence of a catalytic surface saturated in hydrogen. But how can we explain such situation when the temperature is increased? The only way to interpret this result is to consider that, at high temperature, the reaction is only acid-controlled.

Iglesia et al. [17] suggested, to explain a reaction order in hydrogen of +1 for nC_7 conversion at 200 °C, that isomerization occurs by direct reaction of alkanes on acid sites assisted by the presence of metal sites. Pt converts molecular hydrogen into active hydride species, which transfer to the adsorbed carbenium ions on the acidic site. The hydride species shorten the residence time of the carbenium ions on the SZ surface. This accounts for a positive effect of hydrogen. Comelli et al. [31] explained a positive order in hydrogen pressure on *n*-hexane conversion at 200 °C by the fact that hydrogen inhibits catalyst deactivation and that there is a limiting action of hydrogen on the lifetime of reaction intermediates on the catalyst surface. Otherwise, Duchet et al. [32,33] investigated nC_6 on 0.3 wt.% Pt/SZ at 150 °C. Hydrogen had a positive effect on the reaction in a range of pressures from 760 to approximately 4000 Torr. They supposed that a classical bifunctional mechanism is improbable at 150 °C, and that the catalyst, more likely, operates

by an acid mechanism. Therefore, they suggested a mechanism involving Lewis sites in which hydride abstraction from *n*-hexane on coordinatively unsaturated zirconium atoms creates carbenium ions, which adsorb on Lewis basic sites (bridged oxygen atoms). The adsorbed carbenium ions are then rapidly isomerized and finally desorbed by the hydride species. These hydrides are provided by homolytical dissociation of molecular hydrogen on Pt and by spillover of hydrogen atoms on SZ, where they are converted to ($Zr–H^-$). Protons are also formed ($O–H^+$). In this manner, hydrogen increases the concentration of hydride species, accelerates the desorption of carbenium ions and thus the overall reaction rate. This explains the positive order. Following the same idea, Hattori and coworkers [5,19,20] proposed that hydrogen is a source of Brønsted acidity. Molecular hydrogen dissociates on Pt to hydrogen atoms, which migrate by spillover to the SZ sites where they convert to an H^+ and an e^- or H^-. Furthermore, the bifunctional catalysis would be negligently small.

4.3. Reaction orders in n-heptane partial pressure

In general, a bifunctional catalyst exhibits a hydrocarbon reaction order of 1. Tomishige et al. [7] showed a reaction order in *n*-butane of 1.0–1.1, concluding that the butane isomerization is a monomolecular mechanism. However, for Sachtler and coworkers [23], the orders in nC_4, for the rate of iC_4 formation, were between 1.2 and 1.6, depending on temperature and hydrogen pressure. They suggested then an intermolecular mechanism involving a C_8 intermediate. The same experiments have been carried on with nC_5, by Sachtler and coworkers [24], and they found a reaction order of 1.1, in agreement with an intramolecular mechanism. Experiments on nC_6, led by Duchet et al. [32,33], gave also a reaction order of 1. However, Iglesia et al. [17] were far from these results. They investigated nC_7 conversion on 0.4 wt.% Pt/SZ at 200 °C and displayed an almost constant reaction order of 0.2, remarking that this result differs significantly from that observed for alkane reactions on conventional bifunctional catalyst.

In our case, the *n*-heptane reaction order is 1, and reaction temperature and hydrogen pressure do not influence this value: Pt/SZ behaves as a bifunctional catalyst. We have been able to explain this value whatever the hydrogen pressure is. But at high hydrogen pressures, an inhibiting effect was taken into account. This inhibiting effect was equal to $-\beta(Z+1)$. The global hydrocarbon order was then equal to $1-\beta(Z+1)$, depending on the value of β. At low β values, the global order is not far from unity.

Table 5
Apparent activation energy values in *iso*-butane formation over Pt/SZ, according to the results of Tomishige et al. [7]

Partial pressures ratio (H_2/nC_4)	Apparent activation energy (kcal/mol)	
	267–300 °C	220–267 °C
9	9.8	21.7
29	17.9	24.1
99	20.8	25.1

4.4. The apparent activation energy values

It is always puzzling to correlate the influence of the partial pressures of the reactants to the changes in the apparent activation energy values. Tomishige et al. [7] observed, for nC_4 isomerization, an increase in the apparent activation energy values with the increase of the ratio H_2/nC_4 (Table 5). They explained this evolution by the detrimental effect of hydrogen pressure. Moreover, they ascribed, to the difference of apparent activation energy values between the two temperature ranges, a change of reaction mechanism or of the rate determining step. This suggestion could be adapted to our results. Indeed, as observed above, at high hydrogen pressures, the reaction mechanism is different than the one occuring at low pressures. Moreover, the enhancement in hydrogen concentration has a non-beneficial effect on the reaction rate in the high pressure range. The lower values of the apparent activation energies at 1500 and 2250 Torr can be justified by a change in the reaction mechanism. At low pressure, the mechanism is “bifunctional type”, for which the active site is a metal–proton adduct: the apparent activation energy values correspond to those expected for a bifunctional catalyst (∼30 kcal/mol). At pressures higher than 760 Torr, the excess of hydrogen provokes a shift in the reactivity from the metallic part of the adduct to the acidic one. In this case, the apparent activation energy values are decreased due either to higher heat of adsorption than on the metallic sites

or to the presence of more elementary steps in the process. Our values, E_A and E_A^{isom}, are close to those observed by Coman et al. [46] for *n*-hexane conversion on SZ at 120–140 °C: 7–19 kcal/mol, depending on the preparation and on the calcination of catalyst. The rate constant k appearing in Eqs. (2)–(4) is expected to obey the Arrhenius equation while the temperature dependency of the equilibrium constants K_i will follow the Van't Hoff relationship. Then, from the Temkin formula [47] giving the relation between the apparent activation energy (E_A) and the true activation energy (E^0) of heterogeneous reactions, we can write:

$$E_A = E^0 + \sum_i \Delta H_i \quad (5)$$

where ΔH_i are the enthalpies linked to the equilibrium constants K_i. At that point, we can determine the apparent activation energy values from the Eqs. (3) and (4), by using equation $k = Ae^{-E_A/RT}$ and ploting $\ln(k)$ versus $1/T$. Based on the Eq. (5), the enthalpy contribution at high hydrogen pressure will be greater than at low pressure, and as a consequence, the apparent activation energy value at high pressure will be lower than at low pressure [48].

5. Conclusion

Platinum supported sulfated zirconia is a bifunctional catalyst, for which the active site is a metal–proton adduct, more exactly a hydrogen–platinum–proton adduct $[H–(Pt_m)(H^+)_x]^{x+}$. We have proposed that the first surface reaction, the adsorption step, is an associative reaction. The kinetic study of *n*-heptane conversion displays original characteristics: (i) the hydrogen pressure reaction orders are negative at low pressures, while they are positive at high pressures; (ii) the reaction orders versus hydrocarbon are equal to 1, independently of the experimental conditions; (iii) the apparent activation energy values are divided by a factor of 2 when increasing the pressure from atmospheric pressure to higher pressures. We have been able to interpret these results by taking into account the presence of an hydrocarbon inhibiting effect at high pressure. Moreover, these particular behaviors of Pt/SZ were explained by the occupation of platinum–proton adduct site. Hence, at hydrogen pressures higher than 760 Torr, the excess of hydrogen provokes a shift in the reactivity from the metallic part of the adduct to the acidic one. The hydrocarbon is activated by the metallic function of the platinum–proton adduct at low pressures, and by the acidic site at high pressures and at high temperatures. Furthermore, we noticed, from carbon-13 labeled hydrocarbons, that only one carbon–carbon bond breaking reaction takes place during the catalytic process; no scrambling of the ^{13}C is observed. It underlines that no repetitive process occurs. This result will be discussed in a next publication [48].

References

[1] M. Hino, S. Kobayashi, K. Arata, J. Am. Chem. Soc. 101 (1979) 6439.
[2] M. Hino, K. Arata, J.C.S. Chem. Commun. (1980) 851.
[3] J.C. Yori, J.C. Luy, J.M. Parera, Appl. Catal. 46 (1989) 103.
[4] F. Garin, D. Andriamasinoro, A. Abdulsamad, J. Sommer, J. Catal. 131 (1991) 199.
[5] K. Ebitani, J. Konishi, H. Hattori, J. Catal. 130 (1991) 257.
[6] J.M. Grau, J.C. Yori, J.M. Parera, Appl. Catal. A 213 (2001) 247.
[7] K. Tomishige, A. Okabe, K. Fujimoto, Appl. Catal. A 194 (2000) 383.
[8] S.Y. Kim, J.G. Goodwin, S. Hammache, A. Auroux, D. Galloway, J. Catal. 201 (2001) 1.
[9] G.A. Mills, H. Heinemann, T.H. Milliken, A.G. Oblad, Ind. Eng. Chem. 45 (1953) 134.
[10] Ü.B. Demirci, F. Garin, Catal. Lett. 76 (2001) 45.
[11] X. Bai, W.M.H. Sachtler, J. Catal. 129 (1991) 121.
[12] W.M.H. Sachtler, Z. Zhang, Adv. Catal. 39 (1993) 129.
[13] H. Liu, G.D. Lei, W.M.H. Sachtler, Appl. Catal. A 137 (1996) 167.
[14] T.J. McCarthy, G.D. Lei, W.M.H. Sachtler, J. Catal. 159 (1996) 90.
[15] J.-M. Manoli, C. Potvin, M. Muhler, U. Wild, G. Resofszki, T. Buchholz, Z. Paál, J. Catal. 178 (1998) 338.
[16] T. Buchholz, U. Wild, M. Muhler, G. Resofszki, Z. Paál, Appl. Catal. A 189 (1999) 225.
[17] E. Iglesia, S.L. Soled, G.M. Kramer, J. Catal. 144 (1993) 238.
[18] K. Ebitani, H. Konno, T. Tanaka, H. Hattori, J. Catal. 135 (1992) 60.
[19] K. Ebitani, J. Tsuji, H. Hattori, H. Kita, J. Catal. 135 (1992) 609.
[20] T. Shishido, H. Hattori, Appl. Catal. A 146 (1996) 157.
[21] F. Garin, L. Seyfried, P. Girard, G. Maire, A. Abdulsamad, J. Sommer, J. Catal. 151 (1995) 26.
[22] V. Adeeva, G.D. Lei, W.M.H. Sachtler, Catal. Lett. 33 (1995) 135.
[23] H. Liu, V. Adeeva, G.D. Lei, W.M.H. Sachtler, J. Mol. Catal. A 100 (1995) 35.
[24] H. Liu, G.D. Lei, W.M.H. Sachtler, Appl. Catal. A 146 (1996) 165.

[25] M.-T. Tran, N.S. Gnep, M. Guisnet, P. Nascimento, Catal. Lett. 47 (1997) 57.
[26] J.H. Sinfelt, Adv. Chem. Eng. 5 (1964) 37.
[27] F. Chevalier, M. Guisnet, R. Maurel, C.R. Acad. Sci. Ser. C 282 (1976) 3.
[28] M. Belloum, C. Travers, J.P. Burnonville, Rev. Inst. Fr. Pet. 46 (1991) 89.
[29] M. Guisnet, V. Fouche, Appl. Catal. 71 (1991) 295.
[30] A. Sayari, Y. Yang, X. Song, J. Catal. 167 (1997) 346.
[31] R.A. Comelli, Z.R. Finelli, S.R. Vaudagna, N.S. Fígoli, Catal. Lett. 45 (1997) 227.
[32] J.-C. Duchet, D. Guillaume, A. Monnier, J. van Gestel, G. Szabo, P. Nascimento, S. Decker, Chem. Commun. (1999) 1819.
[33] J.-C. Duchet, D. Guillaume, A. Monnier, C. Dujardin, J.P. Gilson, J. van Gestel, G. Szabo, P. Nascimento, J. Catal. 198 (2001) 328.
[34] D. Tichit, B. Coq, H. Armendariz, F. Figuéras, Catal. Lett. 38 (1996) 109.
[35] H. Armendariz, B. Coq, D. Tichit, R. Dutartre, F. Figuéras, J. Catal. 173 (1998) 345.
[36] L. Guczi, A. Frennet, V. Ponec, Acta Chim. Hung. 112 (1983) 127.
[37] A. Frennet, in: Z. Paál, P.G. Menon (Eds.), Hydrogen Effects in Catalysis, Marcel Dekker, New York, 1988, p. 399.
[38] F. Garin, F.G. Gault, J. Am. Chem. Soc. 97 (1975) 4466.
[39] F. Garin, F.G. Gault, G. Maire, Nouv. J. Chim. 5 (1981) 553.
[40] F. Garin, G. Maire, F.G. Gault, Nouv. J. Chim. 5 (1981) 563.
[41] A. Frennet, G. Lienard, A. Crucq, L. Degols, J. Catal. 53 (1978) 150.
[42] A. Frennet, Catal. Today 12 (1992) 131.
[43] P. Parayre, V. Amir-Ebrahimi, F.G. Gault, A. Frennet, J.C.S. Faraday I 76 (1980) 1704.
[44] A. Frennet, G. Lienard, Surf. Sci. 18 (1969) 80.
[45] A. Frennet, G. Lienard, J. Chim. Phys. 68 (1971) 1526.
[46] S. Coman, V. Pârvulescu, P. Grange, V.I. Pârvulescu, Appl. Catal. A 176 (1999) 45.
[47] M. Temkin, Acta Physicochim. U.R.S.S. 2 (3) (1935) 313.
[48] Ü.B. Demirci, Thesis, University of Strasbourg I, June 2002.